SICEL VII Simposio Internacional sobre Calidad de la Energía Eléctrica 2013

Synchronization to the grid using linear Kalman Filter applied to single-phase inverters

O. Carranza, C. L Trujillo, R. Ortega, J. Rodríguez,

***Abstract*— This paper presents the analysis and implementation of a synchronizer to the grid. The synchronizer is developed by Linear Kalman Filter. The synchronizer is used in a single-phase inverter to the grid. This inverter is applied in an environment of microgrids with renewable energy sources (photovoltaic, wind, fuel cell, etc.). The main purpose of the synchronizer is to obtain the phase of the grid. The main objective of obtaining the phase of the grid is to achieve a power factor close to unity in the inverter. This allows to obtain a power factor close to unity in the inverter. Linear Kalman filter is a reduction in Extended Kalman Filter. The analysis of the Extended Kalman Filter is presented. This allows to know the characteristics of the extended Kalman filter and get linear Kalman filter to be used as synchronizer to the grid. Due to the single-phase inverter and Linear Kalman Filter uses a stationary reference frame is required to create an orthogonal system. Orthogonal system is created with an all-pass filter. To compare the results is implemented a synchronizer using PLL, because it is the most used.**

***Index Terms*— Kalman Lineal Filter; PLL; Single-phase Inverter; microgrid.**

I. Introduction

At present, renewable energy sources have a great impact on society because they are energy sources that do not pollute the environment, in addition to the cost of oil is becoming more expensive, which affects the cost of energy electric, also producing a high pollution. The renewable energy sources that currently have a major impact on both the commercial and research are the photovoltaic, wind, and hydrogen, among others. These may be added to the power contribution of the grid and if necessary can work autonomously, providing power directly to the user. Under this perspective, is to make more flexible power distribution schemes already exist. These new generation schemes, called Distributed Generation (DG) [1]-[2]. In this context, generation systems are divided into two types: generation systems that inject directly into the grid (grid connection operation). And generation systems with isolated loads from the grid (island mode operation). These systems are known as microgrid [3].

In systems based on renewable energy generation, energy is obtained in AC or DC, but in most cases is never constant. Therefore, are required one or several stages, which allow energy to be injected into the network. One of the stages, it is a converter AC/DC or converter DC/DC that maintain constant voltage. Then place a DC/AC converter (inverter), which provides the appropriate values of voltage, current and frequency so that the energy is delivered to the grid in the best conditions. Given this condition, the inverter is responsible for regulating the voltage of the DC link, so as to regulate the current that is injected to the grid, and that is in phase with the grid [4]-[5]. The inverter output is placed a low-pass filter components to reduce the switching frequency, typically L filters are used, however, the trend is to use LCL filters having a higher order, the problem with these filters is its resonance frequency which can cause stability problems, so that it requires a more delicate control design [6].

To achieve a power factor close to unity is due to use a stage that enables synchronization of the output current of the inverter to the grid voltage, this provides a sinusoidal current reference. The most used method is a Phase Locked Loop (PLL) [6]. However, in this paper presents the study of synchronization to the network using a linear Kalman filter to analyze its characteristics and set it as a highly viable alternative in synchronization with the grid. The Extended Kalman Filter (EKF) [7]-[8] and the linear Kalman filter (LKF) has been widely used in estimates of speed and position in permanent magnet synchronous motors [9]-[10] and permanent magnet synchronous generators, [11]-[12]. This paper presents the analysis of the EKF, to understand its full operation. This allows reduction algorithm to obtain the LKF, to be used as a method of synchronization to the grid.

The stages of the current control loop, the control loop voltage and grid filter are outside the scope of the paper, these stages are discussed in [4]-[6].

The inverter that injects energy into the grid is a single-phase inverter with bipolar polarization and LCL output filter. Fig. 1 shows the schematic of the inverter with LCL output filter and the control structure is implemented. The control structure is constituted by synchronization to the grid, the current control loop to the grid and voltage control loop of the DC-Link.

O. Carranza, Departamento de Ciencias e Ingeniería de la Computación, Escuela Superior de Cómputo, Instituto Politécnico Nacional, México, D.F, 07738, México, (e-mail: ocarranzac@ipn.mx),

C. L. Trujillo, Department of Electronic Engineering, Universidad Distrital Francisco José de Caldas. Carrera 7 Nº 40-53 Piso 5, Bogotá, Colombia. Phone number: +005713239300/2506, e-mail: cltrujillo@udistrital.edu.co

R. Ortega, Departamento de Ciencias e Ingeniería de la Computación, Escuela Superior de Cómputo, Instituto Politécnico Nacional, México, D.F, 07738, México, (e-mail: rortegag@ipn.mx),

J. J. Rodríguez, Sección de Estudio de Posgrado e Investigación, Escuela Superior de Ingeniería Mecánica y Eléctrica, Instituto Politécnico Nacional, México, D.F., 07738, México, (e-mail: jjrodriguezr@ipn.mx),

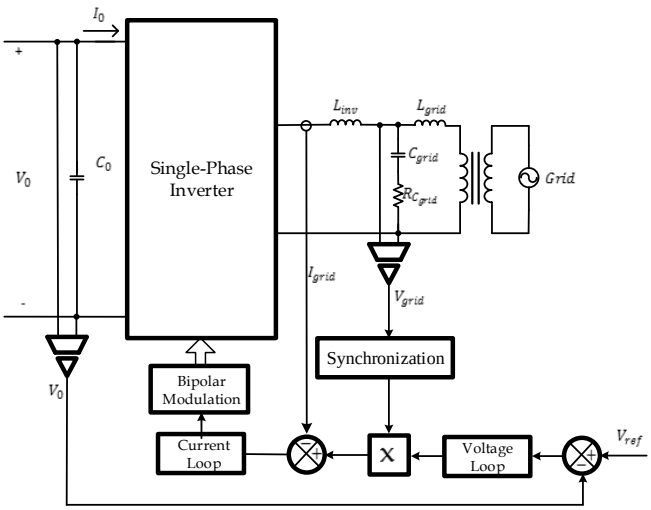

Fig. 1. Diagram of Inverter with LCL output filter and control structure.

II. Generation of Stationary Reference Frame

Synchronization techniques are based on the synchronous reference frame (dp), which is established from stationary reference frame $(\alpha\beta)$ of a three-phase system. However, in this particular case the system is single-phase, so that it should create a signal that allows complete orthogonally signals stationary reference frame. Therefore, it is obtained by

$$V_{grid} = V_{alpha} \tag{1}$$

To create orthogonal signal is performed by

$$V_{\beta} = G_{ort}(s) * V_{\alpha} \tag{2}$$

where

$$G_{ort}(s) = \frac{\omega - s}{\omega + s} \tag{3}$$

$G_{ort}(s)$ is an all-pass filter with a phase shift of the signal from 90 ° to the set frequency (ω), for this case, the signal has a frequency (f) of 50 Hz, therefore, ω is 314.159 rad/s. The Bode diagram of the all-pass filter is shown Fig. 2.

Fig. 3 shows the scheme that is used to create the stationary reference frame.

III. Linear Kalman filter

EKF is analyzed to understand and implement the algorithm as a method of synchronization LKF to the grid.

A. Extender Kalman Filter

EKF [13] is based on the discrete-time lineal dynamic systems, which can be expressed in the form of vectors in the discrete state space, as expressed by (4).

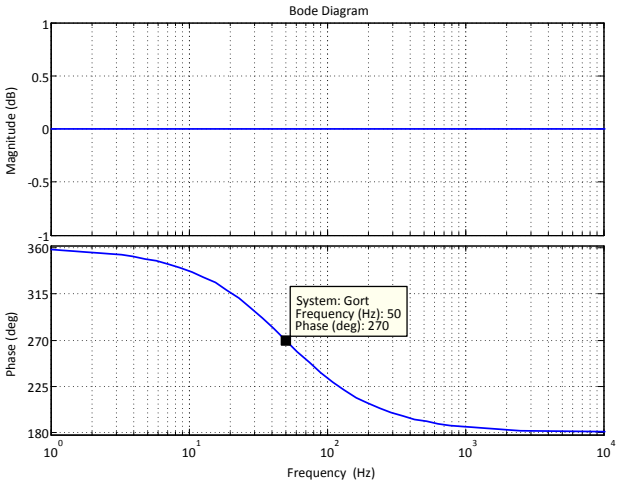

Fig. 2. The bode diagram of the all-pass filter, $G_{ort}(s)$

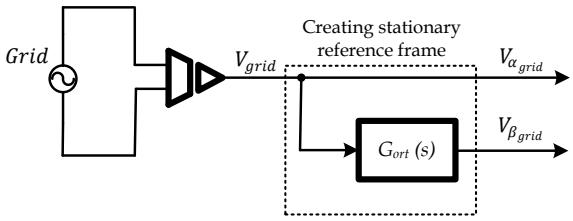

Fig. 3. Scheme for creating stationary reference frame.

$$\begin{aligned} x(k+1) &= A_k x(k) + B_k u(k) + \sigma(k) \\ y(k) &= C_k x(k) + \mu(k) \end{aligned} \tag{4}$$

where y is the output vector and u is the vector of inputs, whereas x is called the state vector. A_k, B_k y C_k are system matrices, which in most cases are obtained from time-varying systems. A system model in discrete time can be obtained by discretization of the continuous time model [14]. σ(t) and μ(t) represents noise and measurement process, with covariance matrices $Q(k)$ and $R(k)$, respectively, noise levels are unknown and act as disturbances of the system, white noise and a stochastic nature. Q and R be regarded as adjustment parameters instead of actual measurements of the noise, in most cases are constants chosen diagonal and through trial and error until the filter works satisfactorily. A third matrix is employed $P(K)$, which represents the error covariance of the state vector.

The EKF algorithm has two steps: estimation and correction. The first step sets a prediction of the state estimation (x_p) and of its covariance matrix (P_p). This is implemented by means of the following recursive relationships:

$$\begin{aligned} x_p(k) &= A_k \tilde{x}(k) + B_k u(k) \\ P_p(k) &= F(k)\tilde{P}(k)F^T(k) + Q \end{aligned} \tag{5}$$

where $F(k)$ is expressed by (6).

$$F(k) = \frac{\partial[A_k\tilde{x}(k) + B_k u(k)]}{\partial x}\bigg|_{x=\tilde{x}(k)} \quad (6)$$

The second step corrects the prediction of the state estimation and that of its covariance matrix by feedback of the measured quantities. This is performed by means of the following recursive relationships.

$$\tilde{x}(k+1) = x_p(k) + K(k)\big[y(k) - C_k(k)x_p(k)\big] \quad (7)$$

$$\tilde{P}(k+1) = P_p(k) - K(k)H(k)P_p(k) \quad (8)$$

where (8) is determined by the Riccati equation of differences (EDR) and $K(k)$ is the gain of the Kalman filter matrix, which is defined by (9).

$$K(k) = P_p(k)H^T(k)\big[H(k)P_p(k)H^T(k) + R\big]^{-1} \quad (9)$$

where $H(k+1)$ is determined by (10).

$$H(k) = \frac{\partial[C_k x(k)]}{\partial x}\bigg|_{x=\tilde{x}(k)} \quad (10)$$

With this set of recursive equations is implemented Extended Kalman filter. The EKF used as the synchronization method to the grid is technically feasible, however, requires a high computational, when implemented in a digital signal processor, therefore is analyzed by the linear Kalman filter.

B. Linear Kalman Filter

To eliminate the problem of high computational, the EKF can be reduced to linear Kalman Filter (LKF) or also known as Kalman Filter Simplified by a number of conditions. The LKF requires a little computational. In the EKF calculates a variable gain matrix *K* (9) which requires a high computational cost. It is an important point in the implementation on a Digital Signal Processor. However, if the filter structure is known, the calculation of K may be reduced to calculate a fixed gain matrix [15]-[17], this results in the LKF.

In the LKF, the state vector is defined by (11).

$$x = \begin{bmatrix} \theta \\ \omega_e \\ \acute{\rho} \end{bmatrix} \quad (11)$$

where θ is the phase angle of the network, ω_e is the angular frequency of the grid and $\rho(k)$ is the process noise with Gaussian distribution with zero mean [15]. In what is considered the following model to calculate the phase angle and the angular frequency, it is expressed by (12)

$$\begin{aligned} \theta(k+1) &= \theta(k) + T_s\omega_e(k) \\ \omega_e(k+1) &= \omega_e(k) + \acute{\rho}(k) \\ \acute{\rho}(k+1) &= \acute{\rho}(k) + \rho(k) \end{aligned} \quad (12)$$

For analysis of this synchronization method, variables are output from the grid voltages in the stationary reference frame, as shown by (13).

$$\begin{bmatrix} y_1(k) \\ y_2(k) \end{bmatrix} = \begin{bmatrix} V_\alpha \\ V_\beta \end{bmatrix} \quad (13)$$

The LKF synchronizer extracts the frequency information from the fundamental component of the grid voltages, whereas other harmonic components are considered as measurement noise. Note that this approach is suitable for this application, because the output voltages contain both low frequency harmonics.

Output variables are sine and cosine of the phase angle, expressed in normalized form to simplify the model and mainly Kalman gain, as shown by (14)

$$\begin{bmatrix} y_1(k) \\ y_2(k) \end{bmatrix} = \begin{bmatrix} \cos\theta(k) \\ \operatorname{sen}\theta(k) \end{bmatrix} + \begin{bmatrix} \mu_1(k) \\ \mu_2(k) \end{bmatrix} \quad (14)$$

where both μ_1 and μ_2 represent switching noise and high-order low frequency harmonics. Considering the state space representation (11) and the input *u(k)=0*, the state space system are rewritten as shown by (15).

$$\begin{aligned} x(k+1) &= A_s x(k) + \rho(k) \\ y(k) &= C_s x(k) + \mu(k) \end{aligned} \quad (15)$$

The expressions of the matrices A_s and $C_s x(k)$ are given by (16) and (17):

$$A_s = \begin{bmatrix} 1 & T_s & 0 \\ 0 & 1 & 1 \\ 0 & 0 & 1 \end{bmatrix} \quad (16)$$

$$C_s x(k) = \begin{bmatrix} \cos\theta(k) \\ \operatorname{sen}\theta(k) \end{bmatrix} \quad (17)$$

Applying (10) to (17) it results (18).

$$H_s(k) = \frac{\partial C_s x(k)}{\partial x} = \begin{bmatrix} -\operatorname{sen}\theta(k) & 0 & 0 \\ \cos\theta(k) & 0 & 0 \end{bmatrix} \quad (18)$$

However, to simplify $H_s(k)$ uses the dq transformation matrix (T) shown by (19).

$$T(\theta) = \begin{bmatrix} \cos\theta & -\operatorname{sen}\theta \\ \operatorname{sen}\theta & \cos\theta \end{bmatrix} \quad (19)$$

$|T(\theta)$ is an orthogonal matrix, ie, $T^T(\theta)T(\theta) = I$. As $H_s(k)$ can be expressed by (20)

$$H_{LKF}(k) = \begin{bmatrix} \cos\theta & \operatorname{sen}\theta \\ -\operatorname{sen}\theta & \cos\theta \end{bmatrix}^T \begin{bmatrix} 0 & 0 & 0 \\ 1 & 0 & 0 \end{bmatrix} \quad (20)$$

where

$$H_s = \begin{bmatrix} 0 & 0 & 0 \\ 1 & 0 & 0 \end{bmatrix} \quad (21)$$

Applying (20) to (9), is obtained simplified filter gain $K_s(k)$, which is shown in (22)

$$K_s(k) = \begin{bmatrix} 0 & K_{s1} \\ 0 & K_{s2} \\ 0 & K_{s3} \end{bmatrix} \begin{bmatrix} \cos\theta(k) & -\text{sen}\,\theta(k) \\ \text{sen}\,\theta(k) & \cos\theta\,(k) \end{bmatrix} \qquad (22)$$

K_{s1}, K_{s2} and K_{s3} are LKF gains that are calculated using the Matlab command DLQE $(A_s, G_s, H_s, Q_s, R_s)$ [18], with the input matrices shown in (23).

$$G_s = R_s = \begin{bmatrix} 0 & 0 & 0 \\ 0 & 0 & 0 \\ 0 & 0 & 1 \end{bmatrix}; \quad Q_s = \delta \begin{bmatrix} 1 & 0 \\ 0 & 1 \end{bmatrix} \qquad (23)$$

In (23) the parameter δ allows to adjust the noise rejection ability, being chosen by trial and error.

With previous development LKF is expressed by (24)

$$\begin{aligned} \varepsilon(k) &= V_\beta(k)\cos\tilde{\theta}(k) - V_\alpha(k)\,\text{sen}\,\tilde{\theta}(k) \\ \tilde{\theta}(k+1) &= \left[\tilde{\theta}(k) + T_s\tilde{\omega}_e(k) + K_{s1}\varepsilon(k)\right]_{-\pi}^{\pi} \\ \tilde{\omega}_e(k+1) &= \tilde{\omega}_e(k) + \acute{\rho}(k) + K_{s2}\varepsilon(k) \\ \acute{\rho}(k+1) &= \acute{\rho}(k) + K_{s3}\varepsilon(k) \end{aligned} \qquad (24)$$

Notably LKF gains are independent of the characteristics of the grid and can be used with different grid conditions. Another advantage of using LKF synchronizer is that the algorithm is very efficient in terms of computational and can be implemented in a Digital Signal Processor without any difficulty.

Fig. 4 shows the scheme of using LKF synchronizer.

Fig. 4. Scheme of synchronizer using a Kalman filter Linear

IV. Results

To compare the results is implemented a synchronizer using PLL [20].

Synchronization method to the grid under study has been evaluated by means of accurate PSIM™ 7.0.5 simulations [19]. Currently working on the design and construction single-phase inverter and control stage with DSP TMS320F28335.

Fig. 5 shows the orthogonal voltages alpha and beta, which are created in the system to synchronize to the grid.

One way to evaluate the response of the synchronizers is applying frequency steps so that the steps are applied grid frequency of 60 Hz to 50 Hz and 60 Hz to 50 Hz, which can obtain the response time of each of synchronizers. Fig. 6 shows the phase behavior of the two synchronizers, When a frequency step is applied to the grid of 60 Hz to 50 Hz, it is observed that the response time of the synchronizer using PLL is 165 ms, corresponding to eight cycles of the grid signal and the response time synchronizer using LKF is 125 ms, which corresponding to six cycles of the grid signal.

Fig. 7 shows the response of the grid voltage when applying a frequency step of the grid of 60 to 50 Hz, which it observed that the voltage generated by each of the synchronizers are placed in phase with the grid voltage.

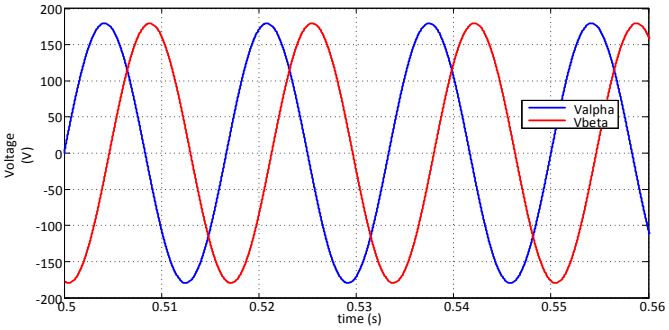

Fig. 5. Alpha and beta Voltages of stationary reference frame.

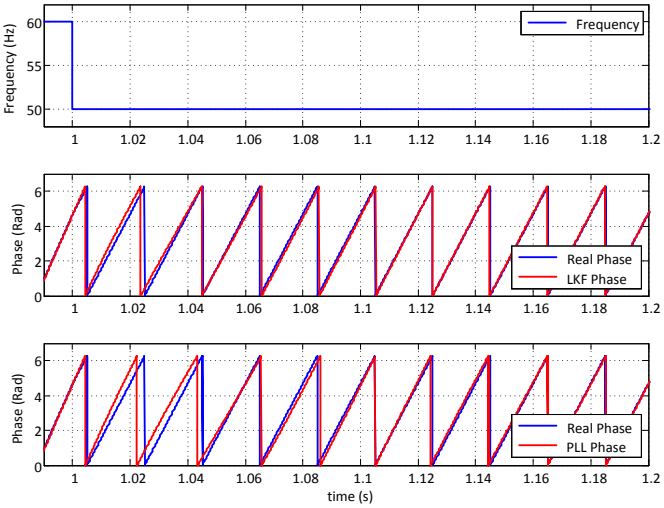

Fig. 6. Behavior of the Phase of a step to the Grid frequency of 60 Hz to 50 Hz.

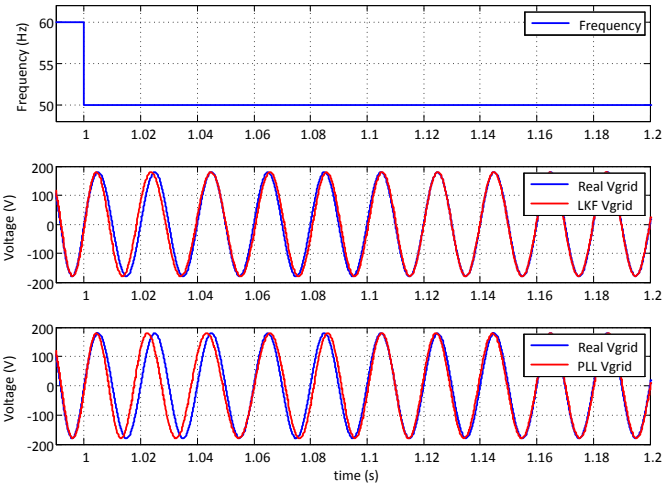

Fig. 7. Behavior of the grid voltage of a step to the Grid frequency of 60 Hz to 50 Hz.

Fig. 8 shows the phase behavior of the two synchronizers, When a frequency step is applied to the grid of 50 Hz to 60 Hz, it is observed that the response time of the synchronizer using PLL is 171 ms, corresponding to ten cycles of the grid signal and the response time synchronizer using LKF is 120 ms, which corresponding to seven cycles of the grid signal.

Fig. 9 shows the response of the grid voltage when applying a frequency step of the grid of 50 to 60 Hz, which it observed that the voltage generated by each of the synchronizers are placed in phase with the grid voltage.

In both cases it is observed that the synchronizer using LKF has a lower response time in comparison with synchronizer using PLL, which in the worst case is 125 ms, and always in six cycles of the grid voltage.

Another evaluation is performed to compare the error between the real voltage and the voltage generated by each of the synchronizers.

Fig. 10 shows the response of the synchronization grid and error signal when applying a frequency step of the grid of 60 to 50 Hz, which is best observed by the error signal when the voltage generated by each of the synchronizers in phase with the grid voltage.

Fig. 11 shows the response of the synchronization grid and error signal when applying a frequency step of the grid of 50 to 60 Hz, which is best observed by the error signal when the voltage generated by each of the synchronizers in phase with the grid voltage.

Fig. 10 and Fig. 11 show that the synchronized using LKF has better behavior.

V. Conclusions

The synchronizer to the grid using a linear Kalman filter has been designed and evaluated in this paper. A stage of creating an orthogonal signal is implemented. Orthogonal signal allows use the stationary reference frame. The synchronizer using LKF has a lower response time in comparison with synchronizer using PLL, which in the worst case is 125 ms, and always in six cycles of the grid signal. Currently working on the design and construction single-phase inverter and control stage with DSP TMS320F28335.

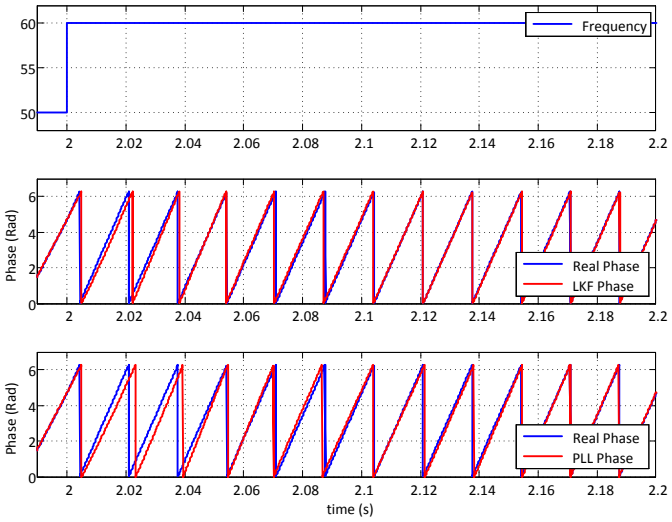

Fig. 8. Behavior of the Phase of a step to the Grid frequency of 50 Hz to 60 Hz.

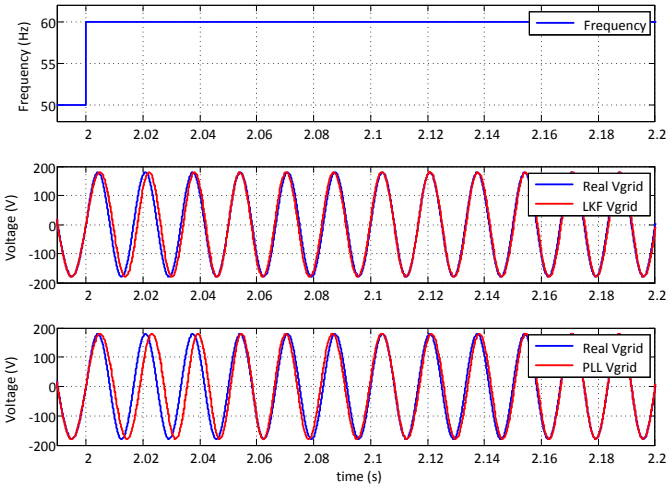

Fig. 9. Behavior of the grid voltage of a step to the Grid frequency of 50 Hz to 60 Hz.

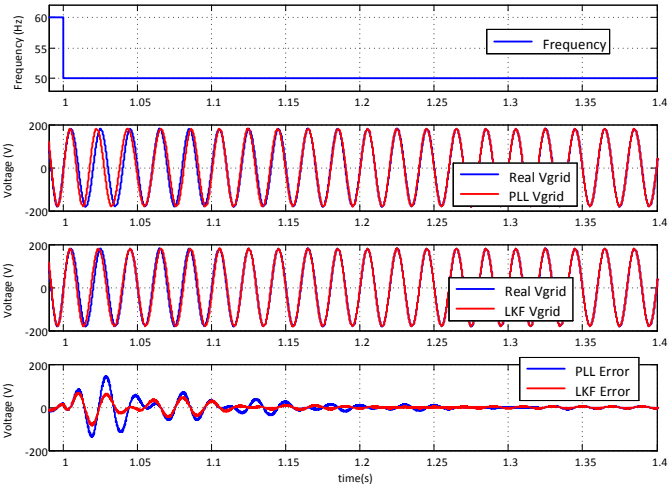

Fig. 10. Behavior of the synchronization grid and error signal of a step to the Grid frequency of 60 Hz to 50 Hz.

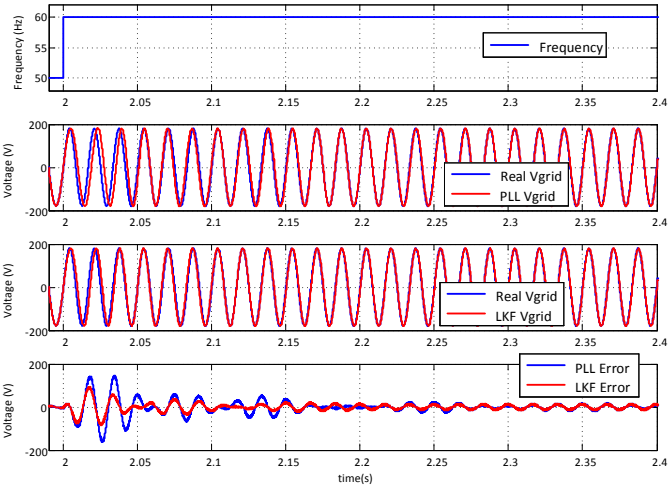

Fig. 11. Behavior of the synchronization grid and error signal of a step to the Grid frequency of 50 Hz to 60 Hz.

REFERENCES

[1] REN21 Steering Committee. "Renewable 2009, Global Status Report, "World watch Institute Washington, DC, 2009.

[2] Puttgen, H.B.; MacGregor, P.R.; Lambert, F.C., "Distributed generation: Semantic hype or the dawn of a new era?", Power and Energy Magazine, IEEE, vol.1, no.1, pp. 22-29, Jan Feb 2003.

[3] Lasseter, R.H., et al. "White paper on integration of distributed energy resources. The CERTS microgrid concept", "Consortium for Electric Reliability Technology Solutions",pp.1-27, 2002.

[4] E. Figueres, G. Garcera, J. Sandia, F. Gonzalez-Espín, J. Calvo, "Sensitivity Study of the Dynamics of Three-Phase Photovoltaic Inverters with an LCL Grid Filter", IEEE Transactions on Industrial Electronics, Vol. 56, No. 3, pp. 706-717, March 2009.

[5] M. Liserre, R. Teodorescu, F. Blaabjerg, "Stability of Photovoltaic an d Wind Turbine Grid-Connected Inverter for a Large Set aof Grid Impedance Values", IEEE Transactions on Power Electronics, Vol. 21, No. 1, pp. 263-272, January 2006.

[6] M. Ciobotaru, R. Teodorescu, F. Blaabjerg, "Control of single-stage single-Phase PV inverter", 11th European Conference on Power Electronics and Applications, EPE '05, pp. 1-10, Sep 2005.

[7] S. Bolognani, L. Tubiana, M Zigliotto, "Extended Kalman Filter Tunning in Sensorless PMSM Drives, IEEE Transactions on Indfustrial Applications, Vol. 39, No. 6, pp. 1741-1747, Nov 2003.

[8] A. Qiu, W. Bin, H. Kojori, "Sensorless control of permanent magnet synchronous motor using extended Kalman filter", Canadian Conference on Electrical and Computer Engineering, pp. 1557-1562, May 2004.

[9] S. Bolognani, R. Oboe, and M. Zigliotto, "Sensorless Full-Digital PMSM Drive With EKF Estimation of Speed and Rotor Position, " IEEE trans. on Industrial Electronics, Vol. 46, No.1, pp. 184-191, February 1999,.

[10] Chan Tze-Fun, P. Borsje, Wang Weimin, "Application of Unscented Kalman filter to sensorless permanent-magnet synchronous motor drive", IEEE International Electric Machines and Drives Conference, IEMDC '09, pp. 631-638, 3-6 May 2009.

[11] L.G. González, E. Figueres, G. Garcerá, O. Carranza, "Maximum-power-point tracking with reduced mechanical stress applied to wind-energy-conversion-systems", Applied Energy, Volume 87, Issue 7, July 2010, Pages 2304-2312. ISSN: 0306-2619.

[12] O. Carranza, E. Figueres, G. Garcerá, L.G. González, "Comparative Study of Speed Estimators with Highly Noisy Measurement Signals for Wind Energy Generation Systems", Applied Energy, Volume 88, (3), pp. 805-813, March 2011.

[13] Chan Tze-Fun, P. Borsje, Wang Weimin, "Application of Unscented Kalman filter to sensorless permanent-magnet synchronous motor drive", IEEE International Electric Machines and Drives Conference, IEMDC '09, pp. 631-638, 3-6 May 2009.

[14] K. Ogata, "Discrete-Time Controls System", Usa, Prentice Hall, 1995.

[15] L. Harnefors, "Speed Estimation From Noisy Resolver Signal," Proceedings of the Sixth International Conference on Power Electronics and Variable Speed Drives, pp. 279-282, 1996;

[16] M.C. Huang, A.J. Moses, F. Anayi, X.G. Yao, "Linear Kalman filter (LKF) sensorless control for permanent magnet synchronous motor based on orthogonal output linear model", International Symposium on Power Electronics, Electrical Drives, Automation and Motion, 2006. SPEEDAM 2006, pp.1381 – 1386, 23-26 May 2006,

[17] Liu Yong, Zhu Zi Qiang, D. Howe, "Instantaneous Torque Estimation in Sensorless Direct-Torque-Controlled Brushless DC Motors", IEEE Transactions on Industry Applications, Vol. 42, No. 5, pp. 1275–1283, Sept.-Oct. 2006.

[18] Matlab 7.6, User´s Guide (2008), MathWork Inc, February 2008.

[19] PSIM 7.0 User´s Guide (2006), Powersim Inc., March 2006.

[20] P. Rodriguez, J. Pou, J. Bergas, J.I. Candela, R.P. Burgos, D. Boroyevich, Decoupled Double Synchronous Reference Frame PLL for Power Converters Control, IEEE Transactions on Power Electronics, Vol. 22, No. 2, pp. 584 – 592, March 2007.

Oscar Carranza received the B.S. degree in Communication and Electronics Engineering from the Instituto Politecnico Nacional, Mexico City, Mexico, in 1996, the M.Sc. degree in Electronics Engineering from the Instituto Politecnico Nacional, Mexico City, Mexico, in 1999, and the Ph.D. degree in Electronics Engineering from the Universidad Politécnica de Valencia, Valencia, Spain, in 2012. He has been professor in Escuela Superior de Computo, Instituto Politecnico Nacional since 1999. His main research fields are in modeling and control of power converters, power processing of renewable energy sources, and grid-connected converters for distributed power.

Rubén Ortega González received the B.Sc. degree in electrical engineering in 1999 and the M.Sc. degree in systems engineering from the Instituto Politécnico Nacional, Mexico, Mexico, and the D.E.A. degree in electrical engineering, computer, and electronic system from the Universidad de Oviedo, Oviedo, Spain, in 2009. He is currently working toward the Ph.D. degree at the Universidad Politécnica de Valencia, Valencia, Spain. He is also currently a Professor with the Department of Computer Science and Engineering, Escuela Superior de Cómputo, Instituto Politécnico Nacional. His main research fields are in modeling and control of power converters applied to the distributed generation in microgrids.